Iraqi Journal of Science, 2026, Vol. 67, No. 10, pp: 5134-5150
DOI: 10.24996/ijs.2026.67.10.3

ISSN: 0067-2904

Utilization of Cigarette Butts Waste as Activated Carbon for Tannin Adsorption in Cigarette Industry Wastewater

Adinda Faisa Mutiara Tsani, Dwi Siswanta, Nurul Hidayat Aprilita*
[1]*Department of Chemistry, Faculty of Mathematics and Natural Sciences, Universitas Gadjah Mada, Yogyakarta, Indonesia*

Received: 28/4/2025 Accepted: 21/12/2025 Published: 30/10/2026

Abstract

The aim of this work is to assess the potential of the cigarette butt waste as KOH-activated carbon (AC-CBW) in removing the tannins from the wastewater of the cigarette industry. The carbonized product was characterized using ATR-FTIR, SEM, SAA, and XRD. After the characterization, the tannin adsorption capacities of AC-CBW were evaluated for different conditions such as adsorbent mass and its contact time with solution, solution pH, and initial tannin concentration. The findings suggest that AC-CBW was amorphous, with a heterogeneous and rough surface topography and a surface area of 143.14 $m^2.g^{-1}$. The detection of hydroxyl (–OH) and carbonyl (C=O) functional groups at 3225 and 1690 cm^{-1}, respectively, were suggestive of the potential to absorb tannins. The highest adsorption efficiency was at 0.3 g adsorbent with 120 min contact time, pH 2, and 20 $mg.L^{-1}$ tannin solution. The experimental adsorption isotherm and kinetic data were best fitted to the pseudo-second-order, Temkin model, and the AC-CBW achieved 86.76% removal efficiency of the tannin from the wastewater of cigarette industry which proves that the adsorbent is effective in the removal of tannins from the textile industry wastewater.

Keywords: activated carbon, adsorption, cigarette butts, tannin

Introduction

The increased sales in the cigarette industry are contributing to social and economic changes around the world. However, with these filters, solid wastes, and other emissions from the cigarette production industry, the industry should also try to implement ways to solve the problem. Wastes from cigarette production, such as filters, are made of materials that are very slow to biodegrade and, as such, are resistant to digestions in soil. Thus, from an environmental perspective, filters released from the wastes of production, contribute serious liability to the ecosystem [1]. Also, from an environmental perspective, the filters, as produced, may contribute serious liability to the ecosystem [2]. Because of these reasons, and from an environmental perspective, very little is of incineration, and loss into a landfill, as traditional waste treatment incineration of waste filters and are also economically costly. This study suggests that these wastes are removed from the ecosystem become a potential material for filter activated carbon, which may serve as an adsorbent.

Because of its high-level ability to adsorb in combination with its multitude of uses in various sectors, activated carbon (AC) is recognized as a multifunctional adsorbent. The

*Email: nurul.hidayat@ugm.ac.id

Open Access Articles. This articles is licensed under

capability of AC to adsorb a wide range of pollutants in both air and water is a factor of its large surface area and specific surface chemistry in addition to its highly porous structure [3]. Additionally, its being an ideal adsorbent is attributed to its affordability, being cost effective, and being eco-friendly with regulatory compliance [4]. The chemical structure of cellulose acetate makes up the majority of the cigarette butts waste (CBW) and given the high carbon content of about ninety-five percent, this waste can serve as a good precursor candidate for producing AC [5]. AC produced from CBW (AC-CBW) has its utmost multifunctionality in its ability to adsorb many contaminants of various pollutants. AC-CBW has a notable capacity for adsorbing the heavy metal Pb^{2+} (lead) and other inorganic pollutants with a qmax of 249.3 $mg.g^{-1}$ [1]. Also, AC-CBW has been shown to adsorb dyes and has an outstanding range of 185–277 $mg.g^{-1}$ and 126–178 $mg.g^{-1}$ in the adsorption of the cationic and anionic, respectively [2].

Carbonized biomass waste via pyrolysis is one among many relevant methods to produce AC (Activated carbon) -CBW (carbonized biomass waste) and its pyrolysis is the chemical decomposition of organic substances at elevated temperatures in the absence of oxygen, consists of gas (CO_2, CO, H_2 and CH_4) and volatile organic compound (bio-oil) products and then solid residues (Char/Carbon) [6]. The carbon material is chemically activated afterwards to remove impurities, re-open, and enhance the pore structure within the AC and further enhance its adsorption products, i.e. contaminants. Chemical activation is generally more effective than its physical counterpart because the activating agent removes the impurities trapped within the global AC structure, leaving behind an activated carbon end product with more available surface area, lower ash content and consumption of process energy [7]. AC-CBW more than one time activated with potassium hydroxide (KOH) presented an outstanding adsorption potential and efficiency for pollutants removal [8].

In the case of the adsorptive uptake of AC-CBW, the adsorbent can treat cigarette industry wastewater by adsorbing the tannin contaminants through the action of both physical adsorption via van der Waals forces and/or chemical bonding of the tannins and AC-CBW [9]. The wastewater tannin results from the soaking of the cloves. Tannin is an organic mixture of different complex polyphenolic compounds containing C, H, and O that can interact to form large macromolecules. The phenolic functional group that makes the polyphenolics polar, and their high aqueous solubility is an important feature of tannins which can also dictate their molecular attributes. The tannin is yellowish white to brown and can undergo darkening when exposed to ultraviolet light or after prolonged exposure to air [10].

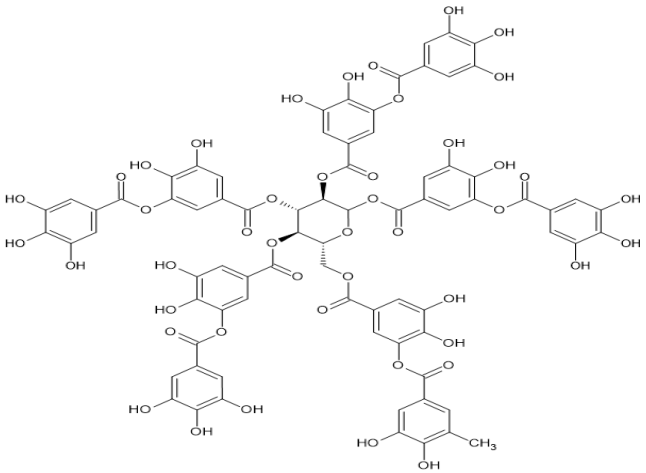

Figure 1: Structure of tannin

Tannins that have escaped into the environment have also caused pollution problems have caused problems for wastewater treatment processes. In nature, tannins have caused discoloration of water, which to be obstructing the photosynthesis of some organisms of an aquatic ecosystem [11]. Furthermore, the high solubility of tannins in water reduces the coagulation efficiency of plant wastewater treatment processes which requires more expensive metal coagulants. This leads to other problems such as metal contamination of the effluent [12]. It has also been shown that tannins are toxic to some microorganisms, which contributes to the inefficiency of some of the biological wastewater treatment processes [13].
The focus of this study is to present a novel technique that is the first of its kind to fully optimize the valorisation of CBW by the production of a chemically activated carbon that targets the removal of tannins from wastewater. The global scholarly attention has paid to the use of various by-products for the production of adsorbents is a stark contrast to the case of CBW where its use for tannins removal is in its infancy. The work outlined the innovative and practical development of an activated carbon, wastes for the provision of a genuinely useful technique for the treatment of wastewater. This initiative promotes a circular economy in industries as it combines the removal of pollutants from the wastewater and the management of solid wastes.

1. Materials and Methods

1.1 Materials

The CBW was used as raw material to prepare the adsorbents. It was collected from PT Djarum in Kudus. The chemicals utilized in this study, including KOH, 37% HCl, tannin, Na_2CO_3, 2 M Folin Ciocalteu reagent, and NaOH, were of at least analytical grade and supplied by Merck. The distilled water utilized in this experiment was supplied by CV Progo Mulyo. Subsequently, wastewater from the cigarette industry, specifically from PT Djarum in Kudus, was utilized for adsorbent applications.

1.2 Preparation of adsorbent materials

The CBWs were air-dried naturally for several days before being stored in a well-ventilated area. The dried CBWs were used as they were in the pyrolysis process at 500ºC for 2 h. After pyrolysis, the carbons (C-CBWs) were washed with distilled water to eliminate dust and other inorganic impurities. Then, they were oven-dried at 110ºC for 12 h to reduce the moisture content and stored in a desiccator. The material obtained was carbon and labelled as C-CBW. The C-CBWs were sieved with a 20 mesh sieve and chemically activated using a 65% KOH solution in a C-CBW/KOH mass ratio of 1:5, followed by impregnation for 24 h [14]. The results of the impregnation were washed with 2 M HCl and distilled water until the supernatant had a neutral pH and filtered with a Buchner filter. The supernatant was oven-dried at 110°C until constant weight. The material obtained was activated carbon and labelled as AC-CBW.

1.3 Characterization of materials

The characterization of materials was performed using several analytical methods. The surface characteristics of both C-CBW and AC-CBW were detected employing an Attenuated Total Reflectance Spectrophotometer-Fourier Transform Infrared (ATR-FTIR) spectrometer. This Spectrophotometer was a Shimadzu OT-IRTrace 100 and obtained spectra at 16 cm^{-1} resolution, from 500 to 4000 cm^{-1}. The XRD patterns of AC-CBW were collected using a Bruker D8 Advance Eco XRD (10-80º). The surface morphologies of C-CBW as well as AC-CBW were documented using a Phenom Desktop ProXL scanning electron microscope. The BET (Brunauer-Emmet-Teller) equation was applied to determine the surface area of C-CBW and AC-CBW, using the isotherms obtained from a Quantachrome Novatouch Lx4.

1.4 Batch adsorption study

The concentrations of tannin in the aqueous solution were quantified using UV-Vis spectrophotometry. To achieve this, a calibration curve was generated from the dilutions of tannin in solution at concentrations of 1 to 50 mg.L^{-1}. The Thermo Scientific Nicolet Aquamate 8100 was the spectrophotometer used, and the λmax (maximum absorbance wavelength) was 762 nm, which was used as the detection wavelength.

The effect of adsorbent dosage, adsorption time, pH solution, and adsorbate concentration on the adsorption of tannin was examined using a batch experiment with tannin standard solutions. In these experiments, the parameter being studied was varied while keeping other conditions constant. The parameters are listed in

Table ***1***. The procedure involved the addition of a known quantity of adsorbent to a 50 mL aqueous solution of adsorbate (tannin standard solution) in a specific pH range contained in a 100 mL glass beaker. The mixture was stirred at a constant rate of 100 rpm for a predetermined duration. An aqueous solution of adsorbate devoid of adsorbent was subjected to testing and designated as the control. The mixture was subsequently filtered using Whatman 40 filter paper. Subsequently, 0.5 mL of the filtrate and 1 M Folin Ciocalteu reagent solution were each transferred into a test tube. Distilled water was added to the test tube in a volume of 7.5 mL, and the contents were stirred until the mixture was homogeneous. Thereafter, the test tube was left to stand for 5 min. Subsequently, 1.5 mL of a 20% Na_2CO_3 solution was added to the test tube and permitted to stand for 30 min at room temperature. The mixture was then analyzed with a UV-Vis spectrophotometer at a maximum wavelength. Following the attainment of optimal conditions for the tannin adsorption process by AC-CBW through batch adsorption studies, AC-CBW will be applied to the tannin adsorption process in cigarette industry wastewater. The removal percentage R (%) of tannin and the amount of tannin adsorbed (qt) by AC-CBW were calculated from the following relations:

$$R(\%) = \frac{C_i - C_f}{C_f} \times 100 \quad (1)$$

$$q_t = \frac{(C_i - C_f) \times V}{m} \quad (2)$$

Where C_i and C_f are the initial concentration and concentration at time t (mg.L^{-1}) of tannin, m is the weight (g) of adsorbent, and V is the volume of tannin solution (L). The data obtained were used to estimate adsorption kinetics and isotherm parameters.

Table 1: Experimental set-up for investigating the effect of process parameters

Operational parameter	Range	Adsorption conditions
Adsorbent dosage	0.01-0.4 g	30 mg.L^{-1} concentration, circumneutral pH (6), contact time 60 min
Adsorption time	0-180 min	30 mg.L^{-1} concentration, circumneutral pH (6), adsorbent dosage 0.3 g
pH solution	1-8	30 mg.L^{-1} concentration, adsorbent dosage 0.3 g, contact time 120 min
Initial adsorbate concentration	1-100 mg.L^{-1}	Adsorbent dosage 0.3 g, contact time 120 min, pH value 2

2. Results and Discussion

2.1 Characterization of AC-CBW

2.1.1 ATR-FTIR characterization of AC-CBW

The Attenuated Total Reflection Fourier Transform Infrared (ATR-FTIR) spectroscopy samples exhibited spectra indicative of activated carbons developed with the activation method employed in this study, as illustrated in Figure 2. Before the initiation of the activation process, the C-CBW spectra exhibited the presence of CO_2 in the gas phase at a wavenumber of 2361 cm^{-1} [15]. The presence of this gas could be attributed to residual CO_2

gas from the pyrolysis process that remained attached to the surface. However, after the activation process, the presence of CO_2 gas in the AC-CBW spectra was no longer observed. This result demonstrates that C-CBW to AC-CBW activation effectively eliminated surface contaminations. Furthermore, the AC-CBW spectra exhibited the presence of new groups, namely -OH and C=O stretching vibrational groups at wave numbers 3225 and 1690 cm^{-1}, respectively [16]. The emergence of these new groups was explained by the presence of vacancies in carbon lattices, generated during CA process that were occluded on further chemical reaction with KOH to -OH group. This has been reported to cause the generation of carbonyl and carboxyl groups on activated carbon [17]. The surface oxygen containing functional groups of AC-CBW might also contribute to its adsorption capacity [18]. These functional groups provide extra sorption sites for pollutants and enhance their attachment [19].

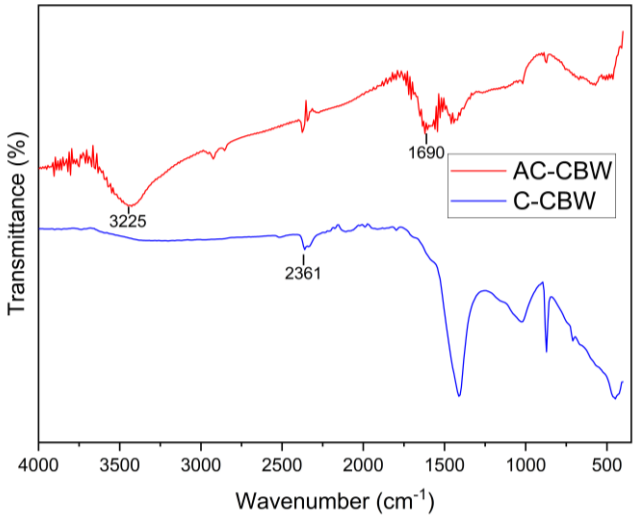

Figure 2: ATR-FTIR spectrum of C-CBW and AC-CBW

2.1.2 Morphological characterization with SEM

Figure 3 and Figure 4 illustrated C-CBW and AC-CBW, respectively. C-CBW showed that the contaminants were attached to the carbon surface, while AC-CBW showed much emptier and expanded pores also a much more aligned surface that contained less contaminants than C-CBW due to the KOH activation. This result showed that KOH activation effectively removed some of the contaminants from the carbon surface. The more enhanced surface for the AC-CBW was attributed to a positive difference on the efficiency of adsorbent to uptake more adsorbate. Less contaminants and more opened pores boosted the overall efficiency of the adsorbent. Moreover, in contrast, the surface of AC-CBW was more heterogeneous and adsorbent surface showed more irregularities and less compact surface overall, which has been recorded in the other studies to enhance the adsorption capacity to large biomolecules of AC [20]. This evenness, low surface compactness and irregularities of AC surface boosted the adsorption capacity of AC-CBW to tannin. The various irregularities in surface structure of the AC possibly increased the efficiency in absorption via providing more active sites needed to enhance the overall adsorption [21]

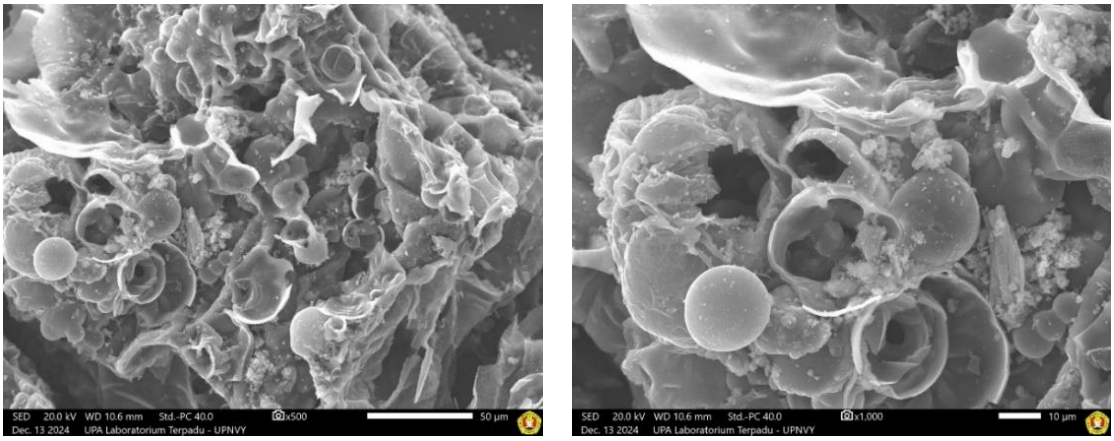

(a) **(b)**

Figure 3: SEM images of C-CBW magnification (a) 500× and (b) 1000×

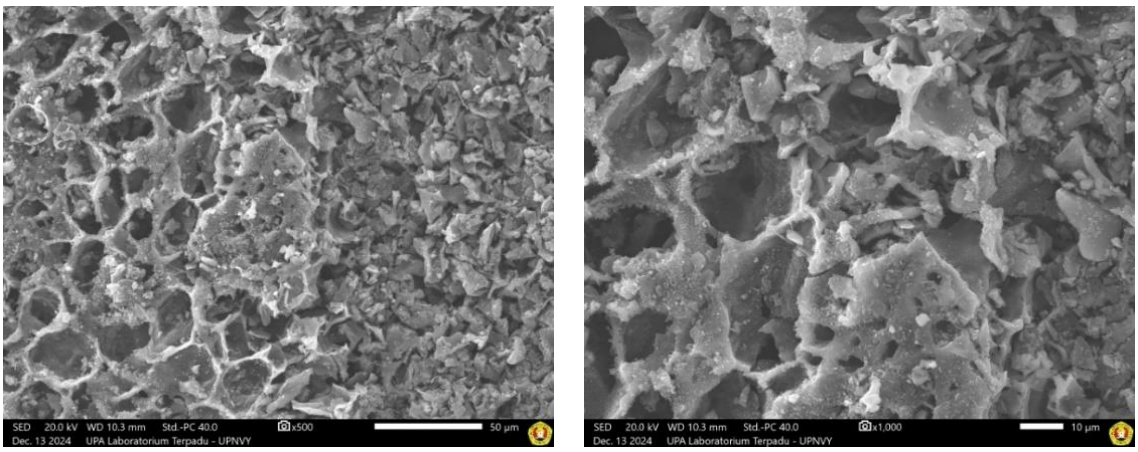

(a) **(b)**

Figure 4: SEM images of AC-CBW magnification (a) 500× and (b) 1000×

2.1.3 Analysis of XRD

The XRD spectrum of the AC-CBW is presented in Figure 5. The XRD pattern of AC-CBW showed that the adsorbent approached to be amorphous with the presence of broad peak at 2θ 20º-30º. This peak is an evidence for the presence of amorphous carbon [22]. However, the presence of crystalline peaks at 2θ = 18.02°, 29.37°, 37.76°, 48°, 53.84°, and 62.65° was also evident. As confirmed with card JCPDS No. 01-071-1166, we found peaks at 2θ = 18.02°, 37.76°, 48°, 53.84°, and 62.65° which indicated anatase TiO_2. TiO_2 in activated carbon could be anticipated due to the inclusion of TiO_2 as a whitening agent in the cigarette filter waste, which underwent pyrolysis and did not decompose due to its thermal stability as noted in the literature [23]. The peak at 2θ = 29.37° proved the presence of kaolin and confirmed with the card JCPDS no. 03-0052. The presence of kaolin in activated carbon could be attributed to the filter waste of cigarette, whereby it constituted the aluminum silicate, a major component of some tobacco products. This aluminum silicate is also thermally stable which explains its presence during the pyrolysis [24]. The analytical results indicated the structure of AC-CBW is predominantly amorphous and the presence of other minerals such as TiO_2 and kaolin are also present in the sample.

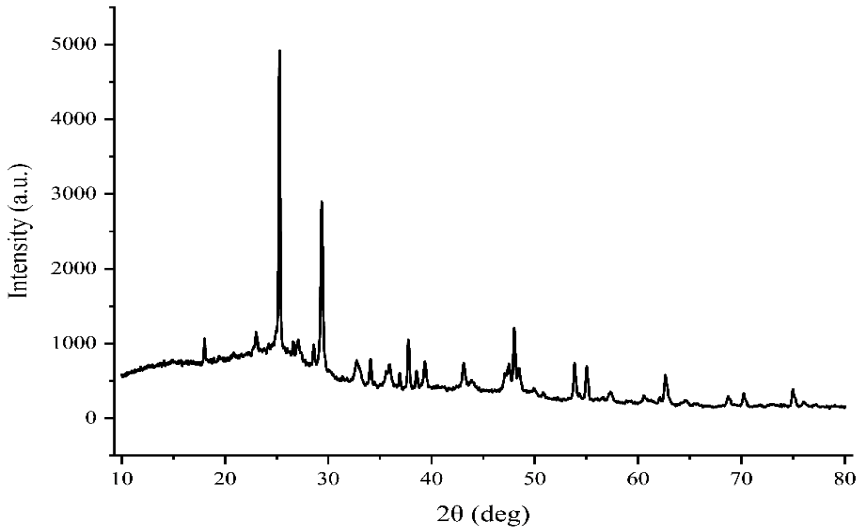

Figure 5: X-ray diffraction pattern of AC-CBW

2.1.4 Specific surface area S_{BET} of AC-CBW

The N_2 adsorption isotherm for AC-CBW may be classified as type II by IUPAC based on the behavior that indicates the adsorbed adsorbate increases as a function of pressure. It is indicative of multilayer physisorption. Presence of such a resorbate sigmoidal II curve is characteristic of the non-porous or macroporous bodies [25]. The corresponding BET specific surface area values for AC-CBW and C-CBW are 143.14 $m^2.g^{-1}$ and 99.74 $m^2.g^{-1}$, respectively. This outcome demonstrated that the activation process of pyrolyzed carbon could enhance the surface area of carbon. The surface area of AC-CBW fell within the range of activated carbon surface area in general, which was 100-2000 $m^2\ g^{-1}$ [26]. Consequently, the enhancement of the specific surface area led to an increase in tannin adsorption. This suggested that materials with the greatest specific surface area might also exhibit the strongest adsorption capabilities.

3.2 The influence of parameters

3.2.1 Effect of adsorbent dosage

The effect of AC-CBW dosage on tannin adsorption was investigated by changing the adsorbent dosage from 0.01 g to 0.4 g in 50 mL of 30 $mg.L^{-1}$ tannin solution at circumneutral pH (6). As depicted in Figure 6, it was evident that with each increase in mass of the adsorbents, there was an increase in the efficiencies of the adsorbents and a decrease in the adsorption capabilities. This was attributed to the excess active surface sites, as there was theoretically a more perfect adsorption occurring with more adsorbent mass. Adsorption efficiencies may have leveled off, however, because of the unoccupied active surface sites where adsorbate was not in contact with the adsorbent mass to equilibrate [27].

This research determined that 0.3 grams of adsorbent mass was optimal. Nevertheless, an increase in adsorbent did not correlate with an increase of adsorption efficiencies. This was likely a result of the balance of the adsorbate that was adsorbed to the surface of the adsorbent compared to the adsorbate that remained in the solution [28]. Therefore, it can be said that there was an added limit to the mass of adsorbent, resulting in non-negligible adsorbate, and a tendency for little to no adsorption efficiencies.

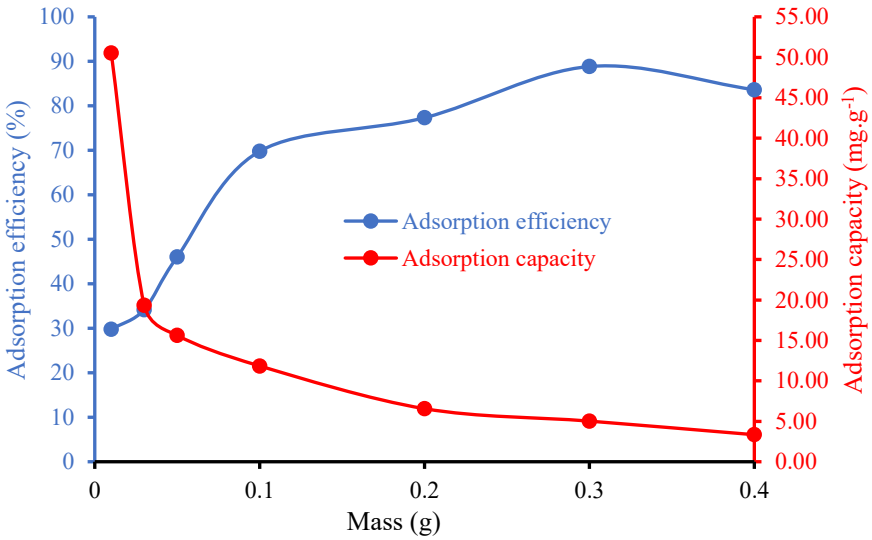

Figure 6: Effect of adsorbent dosage

2.2.2 Effect of contact time

Contact time is one of the important parameters involved in the adsorption process. The contact time was varied between 0 and 180 min using 0.3 g of adsorbent in 50 mL of a 30 mg/L tannin solution at a near-neutral pH of 6. As illustrated by Figure 7, an increase in the contact time increased the efficiency and capacity of tannin adsorption until it attained the optimal value at 120 min. This revealed that during the initial minutes, most of the active sites on the surface of the adsorbent remain unoccupied. As such, the adsorbate showed a tendency to be attracted to the surface of the adsorbent due to the large chemical potential difference between the adsorbent and the solution. This high driving force allowed the adsorbate to easily attach to the surface of the adsorbent [28]. However, with the rise in contact time and a consequential occupation of the active sites, the chemical potential difference became lower, thereby slowing down the rate of adsorption until it achieved a state of equilibrium at a contact time of 120 min. As a result, further extension beyond this time did not result in significant improvement, and it might even cause a reduction in the efficacy of adsorption due to the attainment of equilibrium by the system [29].

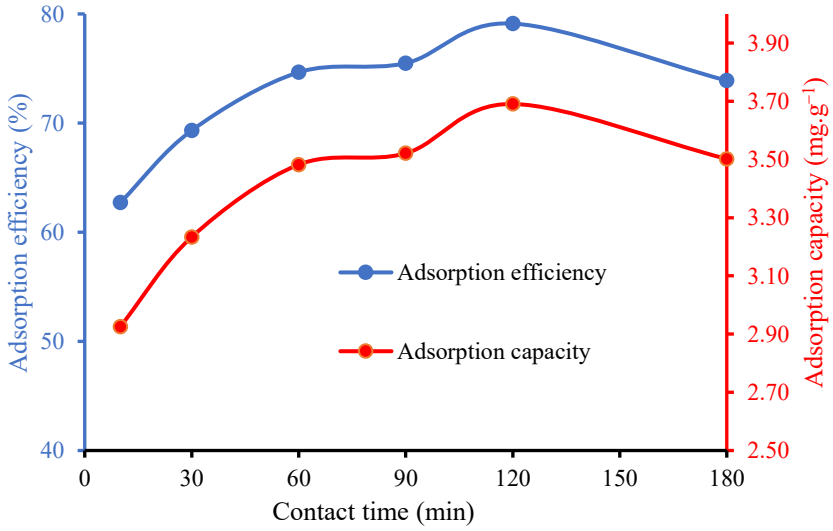

Figure 7: Effect of contact time

2.2.3 Effect of tannin solution pH

Tannin is a weak organic acid and has a high degree of ionization and adsorption in solution because its ionic and adsorption properties are highly dependent upon the surface pH. At pH < 4.5, tannin is predominantly present in the form of neutral molecules. As the solution pH increased, tannin underwent gradual ionization, reaching a state of complete ionization and a negative charge at solution pH >6 [17, 19]. The effect of pH solution on tannin adsorption was investigated by changing the pH solution from 1 to 8 in the adsorption process with 0.3 g of adsorbent in 50 mL of 30 mg.L^{-1} tannin solution for 120 min. Figure 8 indicated that the efficiency and capacity of tannin adsorption decreased with an increase in pH value and was at an optimum with pH 2. This indicated that at solution pH < 4.5, the adsorbent surface would be surrounded with H^+ ions such that its functional groups were positively charged, while tannin remained neutral. Should this occur, it would allow for hydrogen bonding, electrostatic interaction, and π-π interaction of the adsorbent surface with the tannin, as shown in Figure 8. Consequently, this developed the enhancement of its adsorption efficiency and capacity. Conversely, at solution pH >4.5, tannin and the adsorbent surface would be negatively charged, resulting in electrostatic repulsion dominating during the adsorption process, as illustrated in Figure 8. This, in turn, would lead to a reduction in adsorption efficiency and capacity. Conversely, a highly acidic environment (pH 1) inhibited the adsorption process. At this pH, an elevated concentration of H^+ ions competed with tannin ions for binding sites on the adsorbent surface, resulting in reduced tannin adsorption.

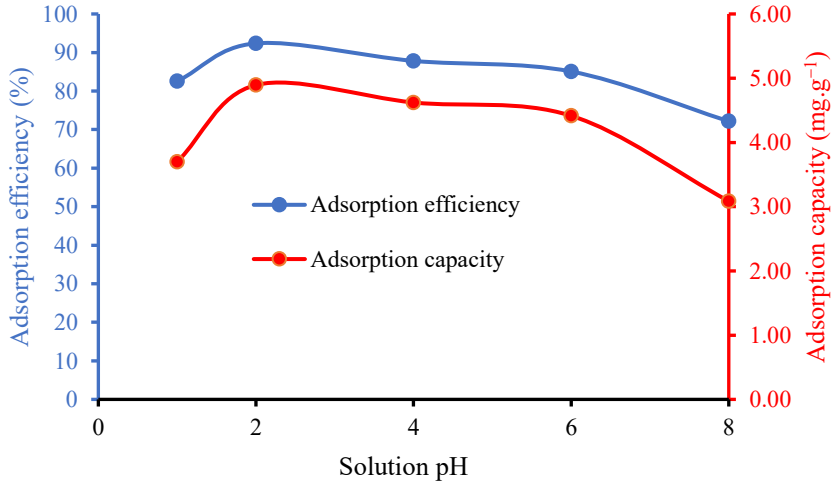

Figure 8: Effect of solution pH

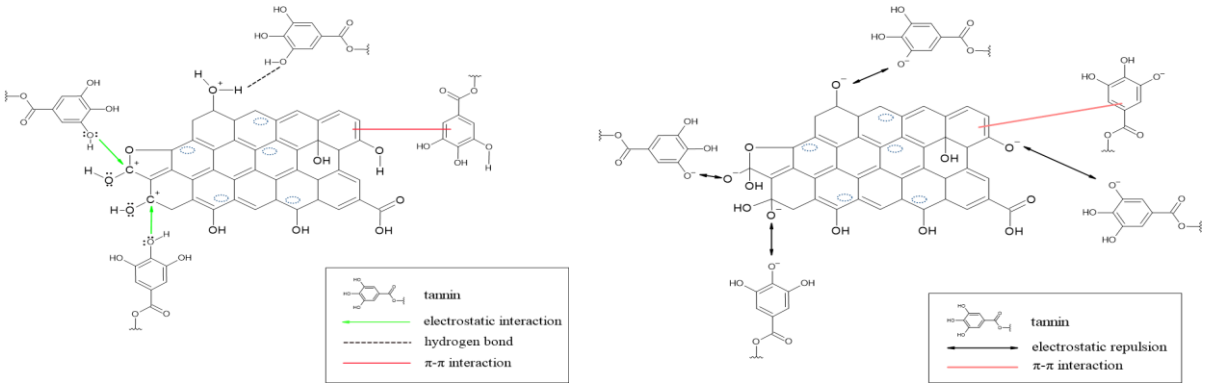

(a) **(b)**

Figure 9: Possible interaction of tannins with AC-CBW at solution pH (a) below 4.5 and (b) above 4.5

2.2.4 Effect of initial tannin concentration

The present study investigated the effect of initial tannin concentration on tannin adsorption. To that end, the concentration was changed from 1 $mg.L^{-1}$ to 100 $mg.L^{-1}$ in the adsorption process with 0.3 g of adsorbent at pH 2 for 120 minutes. As demonstrated in Figure 10, it had been demonstrated that the efficiency of tannin adsorption tended to increase with an increase in the initial concentration of adsorbate, reaching an optimum concentration of 20 $mg.L^{-1}$ with an adsorption capacity of 2.95 $mg.g^{-1}$. Subsequently, a decrease in efficiency was observed. At the onset of the adsorption process, a limited number of adsorbent surfaces were available for binding with the adsorbate. However, once the optimum concentration was attained, a state of equilibrium was achieved among the active sites on the adsorbent surface, due to the saturation of these sites with adsorbate, thereby halting the further increase in adsorbate binding. Moreover, an increase in the initial concentration of adsorbate had been observed to correspond with an increase in the adsorption capacity of tannin. This outcome indicated that an increase in the initial concentration of adsorbate results in a greater number of adsorbate molecules filling the active sites on the surface of the adsorbent, thereby enhancing the adsorption capacity.

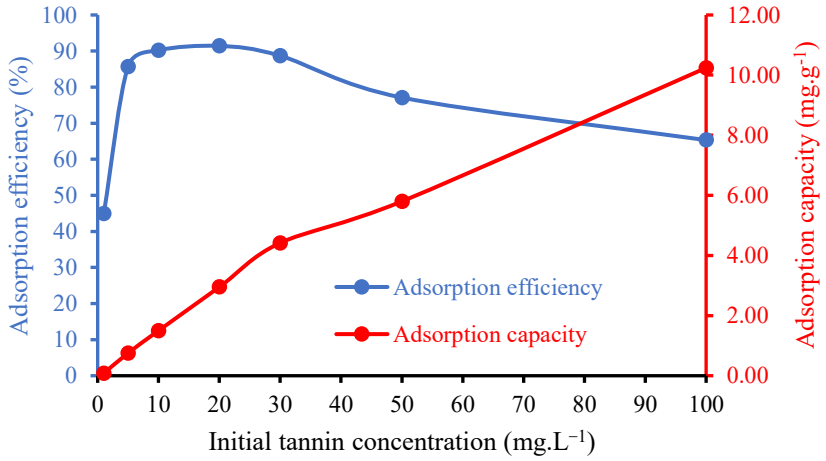

Figure 10: Effect of initial tannin concentration

2.3 Adsorption kinetics

To investigate the rate mechanism of the adsorption process, the adsorption kinetics of AC-CBW were performed, as shown in Figure 11. The pseudo-first-order and pseudo-second-order kinetic models were employed. The linearized forms of pseudo-first-order and pseudo-second-order kinetic models were given as follows.

$$\log(q_e - q_t) = \log q_e - \left(\frac{k_1 t}{2.303}\right) \quad (3)$$

$$\frac{t}{q_t} = \left(\frac{1}{k_2 q_e^2}\right) + \frac{t}{q_e} \quad (4)$$

Where k_1 (min^{-1}) and k_2 ($g.mg^{-1}.min^{-1}$) were the pseudo-first and pseudo-second order rate constants, and q_e ($mg.g^{-1}$) and q_t ($mg.g^{-1}$) were the adsorption capacity at equilibrium and after time t (min). The values of kinetic parameters were reported in Table 2, determined from their respective plots log (q_e-q_t) vs t and t/q_t vs t. The results in Table 2 revealed that adsorption of tannin onto AC-CBW followed the pseudo-second-order kinetics, as the values of R^2 were much higher than the pseudo-first-order. Furthermore, the theoretically obtained tannin adsorption capacity value (3.5971 $mg.g^{-1}$) was close to the experimental value (3.6909 $mg.g^{-1}$), which supported the suitability of the kinetic model [32]. Consequently, it could be concluded that the tannin adsorption process by AC-CBW adheres to a pseudo-second-order adsorption kinetic model, with an adsorption rate constant (K) of 0.1385 $g.mg^{-}1.min^{-1}$. This kinetic model assumed that the adsorption rate was influenced by the diffusion process of

adsorbate into the adsorbent surface, meaning the rate was affected by the interaction between adsorbent and adsorbate.

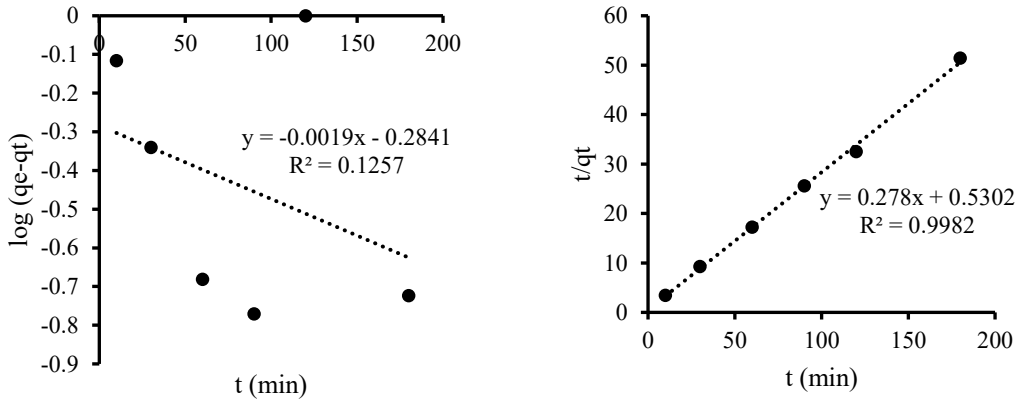

(a) **(b)**

Figure 11: (a) pseudo-first-order and (b) pseudo-second-order kinetic models

Table 2: Kinetics parameters for the adsorption of tannin onto AC-CBW

Adsorption Kinetic Model	Parameters			
	K	q_e cal (mg.g^{-1})	R^2	q_e exp (mg.g^{-1})
Pseudo-first-order	0.0044 min^{-1}	0.5199	0.1257	3.6906
Pseudo-second-order	0.1385 g.mg^{-1}.min^{-1}	3.5971	0.9982	3.6906

2.4 Adsorption isotherms

To optimize design of an adsorption system to remove tannin from solution, it is important to establish the most appropriate correlation for the equilibrium data. The adsorption isotherms could be fitted by Langmuir, Freundlich, Temkin, and Dubinin-Radushkevich models, were performed and shown in Figure 12. The linear equations for the Langmuir, Freundlich, Temkin, and Dubinin-Radushkevich models were as follows.

$$\frac{1}{q_e} = \left(\frac{1}{q_m b C_e}\right) + \frac{1}{q_m} \quad (5)$$

$$\ln q_e = \ln K_F + \frac{1}{n} \ln C_e \quad (6)$$

$$q_e = B_T \ln K_T + B_T \ln C_e \quad (7)$$

$$\ln q_e = \ln q_m - K_{ad} \varepsilon^2 \quad (8)$$

$$\mathrm{E} = \frac{1}{\sqrt{2\mathrm{K_{ad}}}} \quad (9)$$

Where q_e (mg.g^{-1}) and C_e (mg.L^{-1}) were the adsorption capacity and concentration at equilibrium, q_m (mg.g^{-1}) and b (L.mg^{-1}) were Langmuir constants. K_F and n were Freundlich constants, which indicated the capacity and intensity of adsorption. K_T and B were the Temkin isotherm parameters, related to the equilibrium binding constant (L.mg^{-1}) and the heat of adsorption (J.mol^{-1}), respectively. K_{ad} (mol^2.J^{-2}) was the Dubinin-Radushkevich constant, q_m (mg.g^{-1}) was the maximum adsorption capacity, ε was the Polanyi potential, and E (kJ.mol^{-1}) was the adsorption energy. The values of isotherm parameters calculated from their linear plots were mentioned in Table 3. Based on the higher correlation coefficient (R^2) values in Table 3, Temkin model fits much better than the other isotherm models.

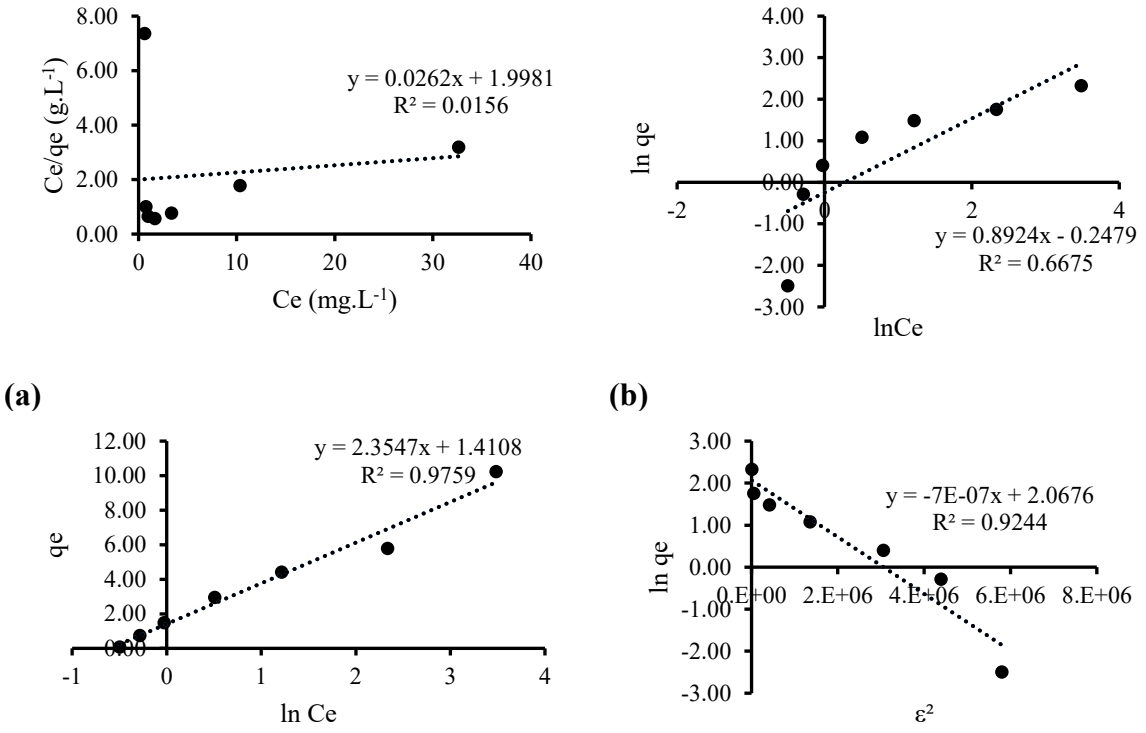

Figure 12: (a) Langmuir, (b) Freundlich, (c) Temkin, and (d) Dubinin-Radushkevich isotherm models

Table 3: Adsorption isotherm parameters for the removal of tannin onto AC-CBW

Isotherm Model	Parameters	Result
Langmuir	q_m	38.1679 mg.g^{-1}
	K_L	0.0131 L.mg^{-1}
	R^2	0.0156
Freundlich	1/n	0.8924
	n	1.1206
	K_F	0.7804 mg$^{1-1/n}$.L$^{1/n}$.g^{-1}
	R^2	0.6675
Temkin	K_T	1.8205 L.mg^{-1}
	B_T	2.3547 J.mol^{-1} or 4.8×10^{-4} kcal.mol^{-1}
	b_T	1059.77
	R^2	0.9759
Dubinin-Radushkevich	q_m	7.9058 mg.g^{-1}
	K_{ad}	7×10^{-7} mol^2.J^{-2}
	E	0.845 kJ.mol^{-1}
	R^2	0.9244

The Temkin isotherm was predicated on the assumption that the heat of adsorption would decrease linearly as the saturation of the adsorbent surface increases [33]. Furthermore, this model posits that the adsorption process was characterized by a uniform and unbounded energy distribution of adsorption sites on a heterogeneous adsorbent surface [34]. The Temkin isotherm model was deemed appropriate in this study, as substantiated by the findings from

the surface morphology SEM characterization, which indicated that the surface of the AC-CBW adsorbent was heterogeneous. In addition, the value of adsorption heat constant (B_T) <1 kcal $mol^{-1,}$ which indicated that the adsorption process occurred by physisorption [35]. The physisorption process allowed for multilayer adsorption on the adsorbent. In the first layer, the adsorbate and adsorbent interacted via hydrogen bonds or π-π interactions. The next layer consisted of π-π interactions between aromatic adsorbates, forming strong van der Waals bonds. Figure 13 shows a proposed mechanism for the multilayer adsorption of tannin molecules onto the surface of the AC-CBW adsorbent.

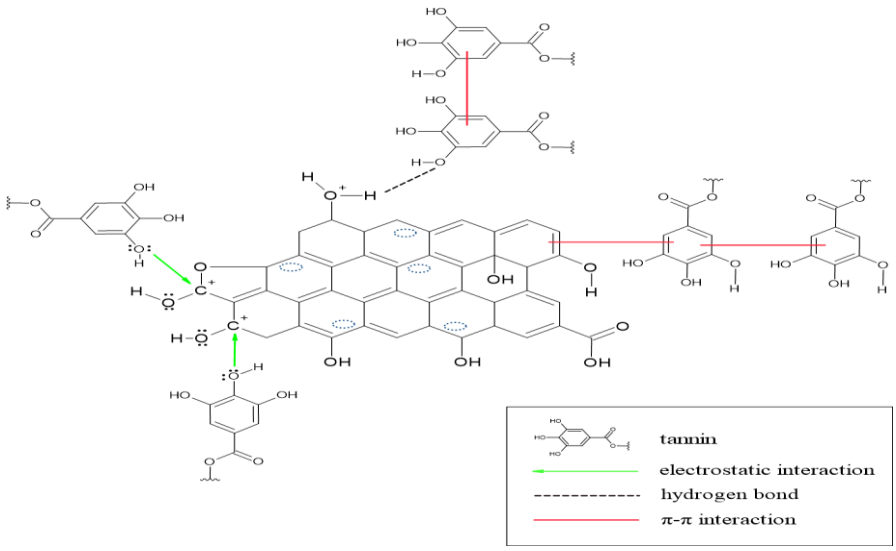

Figure 13: Possible multilayer interaction of tannins with AC-CBW

2.5 Comparison of adsorption capacity of various adsorbents

The adsorption capacities of various adsorbents used for the removal of tannin from aqueous solutions were summarized in Table 4. The maximum multilayer adsorption capacity of AC-CBW was found to be 3.59 $mg.g^{-1}$. As shown in the comparison, the adsorption capacity of AC-CBW was relatively lower than that of several other reported adsorbents.

Table 4: Adsorption capacity of various adsorbents used for the removal of tannin

Adsorbent	Adsorption capacity ($mg.g^{-1}$)	Reference
Calcite	13.36	[36]
Biochar from oil palm frond	67.41	[37]
Carbon steel slag	714.28	[38]
Attapulgite/$CoFe_2O_4$ Magnetic Composites	109.36	[39]
AC-CBW	3.59	This work

However, the adsorbent developed in this study was derived from cigarette filter waste—an abundant yet underutilized material. The synthesis was straightforward and inexpensive, making it appropriate for large-scale applications. Its lower capacity notwithstanding, these benefits highlight the significant potential of AC-CBW as an environmentally friendly and appealing adsorbent, particularly with further refinements (e.g., optimization of the activation process or modification of the surface).

3.5 Application of AC-CBW in the cigarette industry wastewater

In this study we explored AC-CBW in the removal of tannins from wastewaters from the cigarette manufacturing industry. The wastewater used in this study has a pH of 6 and a tannin concentration of 30.65 $mg.L^{-1}$, while the outlet wastewater has a pH of 7 and a tannin

concentration of 2.75 mg.L^{-1}. Under optimal conditions, the tannin concentration in the inlet waste dropped to 4.06 mg.L^{-1} with an adsorption capacity of 4.43 mg.g^{-1} and an efficiency of 86.76. The adsorption of tannins in wastewater by AC-CBW occurred via physisorption and multilayer interactions. This was due to hydrogen bonds, electrostatic interactions, and π-π interactions not involving the transfer or use of shared electrons between the adsorbent and the adsorbate, leading to a physisorption classification. Additionally, π-π interactions occurred between the aromatic rings of tannins that had previously been adsorbed with new tannin molecules, forming the multilayer, as shown in Figure 13. These interactions enhanced the adsorption ability of AC-CBW, resulting in high tannin removal efficiency in wastewater.

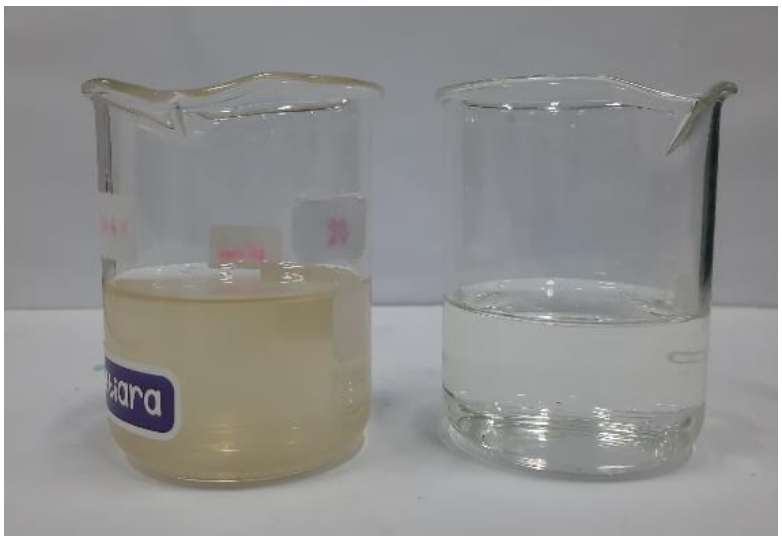

Figure 14: Inlet wastewater before (left) and after (right) AC-CBW adsorbent application

Conclusion

The AC-CBW that was prepared had high surface area, amorphous structure with a mixed surface, and a plethora of O containing functional groups. The optimal conditions for removal were determined to be an adsorbent mass of 0.3 grams, a contact time of 120 minutes, a solution pH of 2, and an initial concentration of 20 mg.L^{-1}. The adsorption of AC-CBW can be explained using pseudo-second-order kinetics and the Temkin isotherm model. This indicates that adsorption is mainly a physical process. The adsorption of tannin with AC-CBW showed good anti-interference properties since successful validation was observed in the wastewater of the cigarette industry, under the optimal parameters found, with a good assessment of stability. There was a marked decrease in tannin from 30.65 mg.L^{-}1 for the initial concentration to 4.06 mg.L^{-1} for the final concentration, producing an adsorption capacity of 4.43 mg.g^{-1}, producing a tanning removal efficiency of 86.76%. In conclusion, the used AC-CBW suffered no waste, showing good performance against simple tannin removal. These advantages are low cost, simple synthesis pathway, rapid equilibrium time and good adsorbent capacity. Providing an environmentally friendly and cheap means of recycling this waste into a usable, recyclable product.

Acknowledgement

This research was supported by the Analytical Chemistry Laboratory, Department of Chemistry, Faculty of Mathematics and Natural Sciences, Gadjah Mada University. The authors express their heartfelt appreciation for their assistance in conducting this research project.

Conflict of Interest

The authors have no conflicts of interest to declare.

References

[1] X. Zhang, M, Yu, Y. Li, F. Cheng, Y. Li, M. Gao, G. Liu, L. Hu, and Y. Liang, "Effectiveness of Discarded Cigarette Butts Derived Carbonaceous Adsorbent for Heavy Metals Removal from Water," *Microchemical Journal*, vol. 168, no. 106474, pp. 1-8, 2021.

[2] A. M. Herrera-gonz, N. Trejo-carbajal, M. C. Reyes-angeles, R. Monroy-galindo, and A. A. Pelaez-Cid, "Activated Carbon Cellulose Acetate Based as Effective Adsorbent of Contaminants from Water," *Colloids Surfaces A: Physicochemical Engineering Aspects*, vol. 694, pp. 1–10, 2024.

[3] C. F. Herrera-puerta, S. Suspes-Garcia, D. M. Galindres-Jimenez, D. Cifuentes-Galindres, L. E. Tinoco, J. C. M. Pirajan, L. G. Gutierrez, and Y. Murillo-Acevedo, "Exploring the Thermal Decomposition of Cigarette Butts and Its Role in Chromium Adsorption Processes," *Heliyon*, vol. 11, no. 42162, pp. 1–15, 2025.

[4] H. Liu, C. Cheng, and H. Wu, "Sustainable Utilization of Wetland Biomass for Activated Carbon Production : A Review on Recent Advances in Modification and Activation Methods," *Science of the Total Environment*, vol. 790, no. 148214, pp. 1-21, 2021.

[5] M. B. Gohain, S. Karki, and P. G. Ingole, "Cellulose Acetate, A Source from Discarded Cigarette Butts for The Development of Mixed Matrix Loose Nanofiltration Membranes for Selective Separation," *International Journal of Biological Macromolecules*, vol. 271, no. 132197, pp. 1–16, 2024.

[6] A. I. Osman, M. Farghali, I. Ihara, A. M. Elgarahy, A. Ayyad, and N. Mehta, "Materials, Fuels, Upgrading, Economy, and Life Cycle Assessment of The Pyrolysis of Algal and Lignocellulosic Biomass : A Review", *Environmental Chemistry Letters,* vol. 21, no. 3. pp. 1419-1476, 2023.

[7] D. Pu, Y. Kou, L. Zhang, B. Liu, W. Zhu, L. Zhu, and T. Duan , "Waste Cigarette Filters: Activated Carbon as a Novel Sorbent for Uranium Removal," *Journal of Radioanalytical and Nuclear Chemistry*, vol. 320, no. 3, pp. 725–731, 2019.

[8] R. E. Elwardany, H. Shokry, A. A. Mustafa, and A. E. Ali, "Influence of of The Prepared Activated Carbon on Cellulose Acetate for Malachite Green Dye Removal from Aqueous Solution," *Macromolecular Research*, vol. 31, no. 11, pp. 1043–1060, 2023.

[9] A. Lim, J. J. Chew, L. H. Ngu, S. Ismadji, D. S. Khaerudini, and J. Sunarso, "Synthesis, Characterization, Adsorption Isotherm, and Kinetic Study of Oil Palm Trunk-Derived Activated Carbon for Tannin Removal from Aqueous Solution," *ACS Omega*, vol. 5, no. 44, pp. 28673–28683, 2020.

[10] Y. Ozogul, Y. Ucar, E. E. Tadesse, N. Rathod, P. Kulawik, M. Trif, T. Esatbeyoglu, and F. Ozogul, "Tannins for Food Preservation and Human Health : A Review of Current Knowledge," *Applied Food Research*, vol. 5, no. 100738, pp. 1–24, 2025.

[11] A. Oliva, C. M. Doolittle, S. A. Medlock, J. F. Aubert, and J. E. Earl, "Effects of Tree Leaves, Tannins, and Water Color on Chlorophyll Concentrations in Ponds," *Hydrobiol.*, vol. 3, no. 3, pp. 263–278, 2024.

[12] E. M. Romero-Dondiz, J. E. Almazán, V. B. Rajal, and E. F. Castro-Vidaurre, "Removal of Vegetable Tannins to Recover Water in The Leather Industry by Ultrafiltration Polymeric Membranes," *Chemical Engineering Research and Design*, vol. 93, pp. 727–735, 2015.

[13] A. Jouali, A. Salhi, A. Aguedach, E. K. Lhadi, M. El Krati, and S. Tahiri, "Photo-catalytic Degradation of Polyphenolic Tannins in Continuous-Flow Reactor using Titanium Dioxide Immobilized on a Cellulosic Material," *Water Science and Technology*, vol. 82, no. 7, pp. 1454–1466, 2020.

[14] J. K. Fatombi, E. A. Idohou, S. A. Osseni, I. Agani, D. Neumeyer, M. Verelst, R. Mauricot, and T. Aminou, "Adsorption of Indigo Carmine from Aqueous Solution by Chitosan and Chitosan/Activated Carbon Composite: Kinetics, Isotherms and Thermodynamics Studies," *Fibers and Polymers*, vol. 20, no. 9, pp. 1820–1832, 2019.

[15] S. Mukhopadhyay, M. S. Naeem, G. S. Shanker, A. Ghatak, A. R. Kottaichamy, R. Shimoni, L. Avran, I. Liberman, R. Bality, R. Ifraemov, I. Rozenberg, M. Shalom, N. Lopez, and I. Hod, "Local CO_2 Reservoir Layer Promotes Rapid and Selective Electrochemical CO_2 Reduction," *Nature Communications*, vol. 15, no. 3397, pp. 1–14, 2024.

[16] V. Anggun and S. Maulina, "Perbandingan Gugus Fungsi dan Morfologi Permukaan Karbon Aktif dari Pelepah Kelapa Sawit Menggunakan Aktivator Asam Fosfat (H_3PO_4) dan Asam Nitrat (HNO_3)," *ST Conference Series*, vol. 1, no. 2, pp. 194–208, 2018.

[17] Y. Zheng, J. Wang, D. Li, C.Liu, Y. Lu, X. Lin, and Z. Zheng, "Insight into The KOH/$KMnO_4$ Activation Mechanism of Oxygen-Enriched Hierarchical Porous Biochar Derived from Biomass Waste by In-Situ Pyrolysis for Methylene Blue Enhanced Adsorption," *Journal of Analytical and Applied Pyrolysis*, vol. 158, no. 105269, pp. 1–16, 2021.

[18] M. Zeinur, R. Pertiwi, E. Delta, and R. Rambu, "Significant Role of Anionic Behavior of Cocoyl Glutamate on Lead (II) Ion Adsorption Towards Activated Carbon Adsorbent from Cigarette Butts," *Case Studies in Chemical and Environmental Engineering*, vol. 11, no. 101140, pp. 1-10, 2025.

[19] W. Dong, J. Xing, Q. Chen, Y. Huang, M. Wu, and P. Yi, "Hydrogen Bonds Between The Oxygen-Containing Functional Groups of Biochar and Organic Contaminants Significantly Enhance Sorption Affinity," *Chemical Engineering Journal*, vol. 499, no. 156654, pp. 1-9, 2024.

[20] A. G. Sethulakshmi and M. P. Saravanakumar, "Reusing Cellulose Acetate Microplastic Fibres Derived from Discarded Cigarette Butts as Superior Adsorbent for Lead Ions: UV Ageing, Adsorption Mechanisms, and DOM Investigation," *Sustainable Materials and Technologies*, vol. 43, no. e01319, pp. 1-18, 2025.

[21] Y. A. B. Neolaka, Y. Lawa, J. Naat, A. C. Lalang, B. A. Widyaningrum, G. F. Ngasu, K. A. Niga, H. Darmokoesoemo, M. Iqbal, and H. S. Kusuma, "Adsorption of Methyl Red from Aqueous Solution using Bali Cow Bones (*Bos javanicus omesticus*) Hydrochar Powder," *Results in Engineering*, vol. 17, no. 100824, pp. 1-10, 2023.

[22] D. Shrestha, "Applications of Functionalized Porous Carbon from Bio-Waste of Alnus Nepalensis in Energy Storage Devices and Industrial Wastewater Treatment," *Heliyon*, vol. 9, pp. 1–12, 2023.

[23] S. A. Arat, "A Review on Cigarette Butts: Environmental Abundance, Characterization, and Toxic Pollutants Released into Water from Cigarette Butts," *Science Total Environmental*, vol. 928, no 172327, pp. 1–12, 2024.

[24] M. R. Fresquez, C. H. Watson, L. Valentin-blasini, and R. S. Pappas, "Characterizing the Transport of Aluminum-, Silicon-, and Titanium-Containing Particles and Nanoparticles in Mainstream Tobacco Smoke," *J. Anal. Toxicol.*, vol. 45, pp. 722–729, 2021.

[25] F. S. Irwansyah, A. I. Amal, E. W. Diyanthi, and E. P. Hadisantoso, "How to Read and Determine the Specific Surface Area of Inorganic Materials using the Brunauer-Emmett-Teller (BET) Method," *ASEAN Journal of Science and Engineering*, vol. 4, no. 1, pp. 61–70, 2024.

[26] D. A. Purbaningrum, A. E. Afiuddin, and T. A. Ramadani, "Pembuatan dan Karakterisasi Karbon Aktif Batang Tembakau (*Nicotiana spp L.*) Sebagai Adsorben," *Conference Proceeding on Waste Treatment Technology*, vol. 5, no. 1, pp. 6–9, 2022.

[27] G. Teng, X. Yuen, and W. Fen, "Adsorption of Pollutants in Wastewater via Biosorbents, Nanoparticles, and Magnetic Biosorbents: A Review," *Environmental Research*, vol. 212, no. 113248, pp. 1-20, 2022.

[28] A. A. G. Khamseh, S. A. Ghorbanian, and Y. Amini, "Investigation of Kinetic, Isotherm, and Adsorption Efficacy of Thorium by Orange Peel Immobilized on Calcium Alginate," *Scientific Reports*, vol. 13, no. 8393, pp. 1–12, 2023.

[29] A. Sasmita and D. Situmeang, "CO Adsorption Performance of Rubber Wood Activated Carbon," *Materials Today: Proceedings*, vol. 63, pp. S26–S31, 2022.

[30] R. Kumar, M. A. Barakat, and E. M. Soliman, "Removal of Tannic Acid from Aqueous Solution by Magnetic Carbohydrate Natural Polymer," *Journal Industrial and Engineering Chemistry*, vol. 20, pp. 2992–2997, 2014.

[31] B. Tang, M. Li, L. Liu, K. Li, J. Xu, J. Ma, and H. Zhang, "Highly Efficient Removal of Tannic Acid from Wastewater using Biomimetic Porous Materials," *Environmental Research*, vol. 252, no. 118252, pp. 1-13, 2024.

[32] H. Motaghi, P. Arabkhani, M. Parvinnia, and A. Asfaram, "Simultaneous Adsorption of Cobalt Ions, Azo Dye, and Imidacloprid Pesticide on The Magnetic Chitosan/Activated Carbon @UiO-66 Bio-Nanocomposite: Optimization, Mechanisms, Regeneration, and Application," *Separation and Purification Technology*, vol. 284, no. 120258, pp. 1-14, 2022.

[33] D. Dermawan, A. Diva, D. Isna, and R. Firnandi, "Case Studies in Chemical and Composite Adsorbent from Sugarcane (*Saccharum officinarum*) Bagasse Biochar Generated from Atmospheric Pressure Microwave Plasma Pyrolysis Process and Nano Zero Valent Iron (nZVI) for Rapid and Highly Efficient Cr (VI) Adsorption," *Case Studies in Chemical and*

Environmental Engineering, vol. 11, no. 101123, pp. 1-15, 2025.

[34] J. Serafin and B. Dziejarski, "Application of Isotherms Models and Error Functions in Activated Carbon CO_2 Sorption Processes," *Microporous and Mesoporous Materials*, vol. 354, no. 112513, pp. 1–19, 2023.

[35] T. Mahajan, S. Paikaray, and P. Mahajan, "Applicability of The Equilibrium Adsorption Isotherms and The Statistical Tools on to Them: A Case Study for The Adsorption of Fluoride onto Mg-Fe-CO_3 LDH," *Journal of Physics: Conference Series*, vol. 2603, no. 012056, pp. 1–13, 2023.

[36] M. Tangarfa, N. Semlali, A. Hassani, and A. Alaoui, "Behavior and Mechanism of Tannic Acid Adsorption on the Calcite Surface: Isothermal, Kinetic, and Thermodynamic Studies," *ACS Omega*, vol. 4, pp. 19647–19654, 2019.

[37] A. A. Lawal, M. A. Hassan, M. A. A. Farid, T. A. T. Yasim-Anuar, M. H. Samsudin, M. Z. M. Yusoff, M. R. Zakaria, M. N. Mokhtar, and Y. Shirai, "Adsorption Mechanism and Effectiveness of Phenol and Tannic Acid Removal by Biochar Produced from Oil Palm Frond using Steam," *Environmental Pollution*, vol. 269, no. 116197, pp. 1–10, 2021.

[38] O. Sarti, F. El Mansouri, E. H. Yahia, E. Otal, and M. Saidi, "Efficient Removal of Tannic Acid from Olive Mill Wastewater Using Carbon Steel Slag," *Journal of Carbon Research*, vol. 9, no. 32, pp. 1–24, 2023.

[39] Y. Teng, Z. Liu, K. Yao, W. Song, Y. Sun, and H. Wang, "Preparation of Attapulgite/$CoFe_2O_4$ Magnetic Composites for Efficient Adsorption of Tannic Acid from Aqueous Solution," *International Journal of Environmental Research and Public Health*, vol. 16, no. 2187, pp. 1–17, 2019.